Second harmonic generation in multi-domain χ^2 media: from disorder to order

Mousa Ayoub,* Jörg Imbrock, and Cornelia Denz

Institute of Applied Physics and Center for Nonlinear Science, Westfälische Wilhelms-Universität Münster, Corrensstraße 2, 48149 Münster, Germany

*ayoubm@uni-muenster.de

Abstract: We investigate systematically the evolution of second harmonic generation in strontium barium niobate with different degrees of disorder of its χ^2 nonlinearity. These different degrees of disordered domain structures are achieved through electrically switching of the polarization at room temperature. The size and distribution of the domains change during the poling process and this in turn strongly affects the spatial distribution of the second harmonic signal. The degree of disorder can be determined by analyzing the angular distribution and wavelength dependence of the second harmonic emission patterns combined with measurements of the spontaneous polarization. We demonstrate evidence of the control of the second harmonic emission pattern by creating defined states of order, and successfully reproduce the resulting patterns theoretically.

OCIS codes: (190.0190) Nonlinear optics; (190.4420) Nonlinear optics, transverse effects in; (190.2620) Harmonic generation and mixing; (160.2260) Ferroelectrics.

References and links

1. M. M. Fejer, G. A. Magel, D. H. Jundt, and R. L. Byer, "Quasi-phase-matched second harmonic generation: Tuning and tolerances," IEEE J. Quantum. Electron. **28**, 2631–2654 (1992).
2. V. Berger, "Nonlinear photonic crystals," Phys. Rev. Lett. **81**, 4136–4139 (1998).
3. I. Freund, "Nonlinear diffraction," Phys. Rev. Lett. **21**, 1404–1406 (1968).
4. G. Dolino, J. Lajzerowicz, and M. Vallade, "Second-harmonic light scattering by domains in ferroelectric triglycine sulfate," Phys. Rev. B **2**, 2194–2200 (1970).
5. M. Baudrier-Raybaut, R. Haidar, P. Kupecek, P. Lemasson, and E. Rosencher, "Random quasi-phase-matching in bulk polycrystalline isotropic nonlinear materials," Nature **432**, 374–376 (2004).
6. P. Molina, S. Álvarez García, M. O. Ramírez, J. García-Solé, L. E. Bausá, H. Zhang, W. Gao, J. Wang, and M. Jiang, "Nonlinear prism based on the natural ferroelectric domain structure in calcium barium niobate," Appl. Phys. Lett. **94**, 071111 (2009).
7. A. S. Aleksandrovsky, A. M. Vyunishev, I. E. Shakhura, A. I. Zaitsev, and A. V. Zamkov, "Random quasi-phase-matching in a nonlinear photonic crystal structure of strontium tetraborate," Phys. Rev. E **78**, 031802 (2008).
8. S. Kawai, T. Ogawa, H. S. Lee, R. C. DeMattei, and R. S. Feigelson, "Second-harmonic generation from needle-like ferroelectric domains in $Sr_{0.6}Ba_{0.4}Nd_2O_6$ single crystals," Appl. Phys. Lett. **73**, 768–770 (1998).
9. F. Sibbers, J. Imbrock, and C. Denz, "Sum-frequency generation in disordered quadratic nonlinear media," Proc. SPIE **7728**, 77280Y (2010).
10. R. Fischer, S. M. Saltiel, D. N. Neshev, W. Krolikowski, and Y. S. Kivshar, "Broadband femtosecond frequency doubling in random media," Appl. Phys. Lett. **89**, 191105 (2006).
11. P. Molina, M. de la O Ramírez, and L. E. Bausá, "Strontium barium niobate as a multifunctional two-dimensional nonlinear photonic glass," Adv. Funct. Mater. **18**, 709–715 (2008).
12. A. R. Tunyagi, M. Ulex, and K. Betzler, "Noncollinear optical frequency doubling in strontium barium niobate," Phys. Rev. Lett. **90**, 243901 (2003).

#143120 - $15.00 USD Received 24 Feb 2011; revised 29 Apr 2011; accepted 1 May 2011; published 26 May 2011

13. K. A. Kuznetsov, G. K. Kitaeva, A. V. Shevlyuga, L. I. Ivleva, and T. R. Volk, "Second harmonic generation in a strontium barium niobate crystal with a random domain structure," JETP Lett. **87**, 98–102 (2008).
14. S. M. Saltiel, D. N. Neshev, R. Fischer, W. Krolikowski, A. Arie, and Y. S. Kivshar, "Spatiotemporal toroidal waves from the transverse second-harmonic generation," Opt. Lett. **33**, 527–529 (2008).
15. R. Fischer, D. N. Neshev, S. M. Saltiel, A. A. Sukhorukov, W. Krolikowski, and Y. S. Kivshar, "Monitoring ultrashort pulses by transverse frequency doubling of counterpropagating pulses in random media," Appl. Phys. Lett. **91**, 031104 (2007).
16. J. Trull, S. Saltiel, V. Roppo, C. Cojocaru, D. Dumay, W. Krolikowski, D. Neshev, R. Vilaseca, K. Staliunas, and Y. Kivshar, "Characterization of femtosecond pulses via transverse second-harmonic generation in random nonlinear media," Appl. Phys. B **95**, 609–615 (2009).
17. D. Dumay, S. M. Saltiel, D. N. Neshev, W. Krolikowski, and Y. S. Kivshar, "Pulse measurements by randomly quasi phase matched second harmonic generation in the regime of total internal reflection," J. Phys. B **42**, 175403 (2009).
18. U. Voelker and K. Betzler, "Domain morphology from k-space spectroscopy of ferroelectric crystals," Phys. Rev. B **74**, 132104 (2006).
19. U. Voelker, U. Heine, C. Gödecker, and K. Betzler, "Domain size effects in a uniaxial ferroelectric relaxor system: The case of $Sr_xBa_{1-x}Nb_2O_6$," J. Appl. Phys. **102**, 114112 (2007).
20. D. V. Isakov, M. S. Belsley, T. R. Volk, and L. I. Ivleva, "Diffuse second harmonic generation under the ferroelectric switching in $Sr_{0.75}Ba_{0.25}Nb_2O_6$ crystals," Appl. Phys. Lett. **92**, 032904 (2008).
21. D. V. Isakov, T. R. Volk, and L. I. Ivleva, "Investigation of ferroelectric properties of strontium barium niobate crystals by second harmonic generation technique," Phys. Solid State **51**, 2334–2341 (2009).
22. T. Volk, D. Isakov, M. S. Belsley, and L. Ivleva, "Switching kinetics of a relaxor ferroelectric $Sr_{0.75}Ba_{0.25}Nb_2O_6$ observed by the second harmonic generation method," Phys. Status Solidi A **2**, 321–325 (2009).
23. D. Viehland, Z. Xu, and W.-H. Huang, "Structure-property relationships in strontium barium niobate I. needle-like nanopolar domains and the metastably-locked incommensurate structure," Philos. Mag. A **71**, 205–217 (1995).
24. P. Lehnen, W. Kleemann, T. Woike, and R. Pankrath, "Ferroelectric nanodomains in the uniaxial relaxor system $Sr_{0.61-x}Ba_{0.39}Nb_2O_6:Ce_x^{3+}$," Phys. Rev. B **64**, 224109 (2001).
25. J. Dec, V. V. Shvartsman, and W. Kleemann, "Domainlike precursor clusters in the paraelectric phase of the uniaxial relaxor $Sr_{0.61}Ba_{0.39}Nb_2O_6$," Appl. Phys. Lett. **89**, 212901 (2006).
26. K. Terabe, S. Takekawa, M. Nakamura, K. Kitamura, S. Higuchi, Y. Gotoh, and A. Gruverman, "Imaging and engineering the nanoscale-domain structure of a $Sr_{0.61}Ba_{0.39}Nb_2O_6$ crystal using a scanning force microscope," Appl. Phys. Lett. **81**, 2044–2046 (2002).
27. V. V. Shvartsman, W. Kleemann, T. Lukasiewicz, and J. Dec, "Nanopolar structure in $Sr_xBa_{1-x}Nb_2O_6$ single crystals tuned by Sr/Ba ratio and investigated by piezoelectric force microscopy," Phys. Rev. B **77**, 054105 (2008).
28. V. Roppo, W. Wang, K. Kalinowski, Y. Kong, C. Cojocaru, J. Trull, R. Vilaseca, M. Scalora, W. Krolikowski, and Y. Kivshar, "The role of ferroelectric domain structure in second harmonic generation in random quadratic media," Opt. Express **18**, 4012–4022 (2010).
29. Y. Le Grand, D. Rouede, C. Odin, R. Aubry, and S. Mattauch, "Second-harmonic scattering by domains in RbH_2PO_4 ferroelectrics," Opt. Commun. **200**, 249–260 (2001).
30. A. Arie and N. Voloch, "Periodic, quasi-periodic, and random quadratic nonlinear photonic crystals," Laser Photonics Rev. **4**, 355–373 (2010).
31. S. Stivala, A. C. Busacca, A. Pasquazi, R. L. Oliveri, R. Morandotti, and G. Assanto, "Random quasi-phase-matched second-harmonic generation in periodically poled lithium tantalate," Opt. Lett. **35**, 363–365 (2010).
32. L. Tian, D. A. Scrymgeour, and V. Gopalan, "Real-time study of domain dynamics in ferroelectric $Sr_{0.61}Ba_{0.39}Nb_2O_6$," J. Appl. Phys. **97**, 114111 (2005).
33. Y. Sheng, J. Dou, B. Ma, B. Cheng, and D. Zhang, "Broadband efficient second harmonic generation in media with a short-range order," Appl. Phys. Lett. **91**, 011101 (2007).
34. K. Megumi, N. Nagatsuma, Y. Kashiwada, and Y. Furuhata, "The congruent melting composition of strontium barium niobate," J. Mater. Sci. **11**, 1583-1592 (1976).

1. Introduction

Second-harmonic generation (SHG) in ferroelectric crystals is one of the best studied nonlinear optical effects. The efficiency of the generation of new optical frequencies depends critically on matching of the phase velocities of the interacting waves. The most versatile technique for so-called quasi-phase matching is to periodically pole ferroelectric crystals, where the phase mismatch is compensated for by a reciprocal grating vector [1]. This concept can be extended to a two-dimensional (2D) modulation of the quadratic nonlinearity [2] called nonlinear photonic

#143120 - $15.00 USD Received 24 Feb 2011; revised 29 Apr 2011; accepted 1 May 2011; published 26 May 2011

crystal. However, the discrete modulation of the nonlinearity only allows for the phase matching of a discrete set of wavelengths. Broadband parametric processes can only be realized in media with a disordered structure of the nonlinearity [3,4] like polycrystalline ferroelectrics [5], and crystals with randomly distributed antiparallel microdomains like calcium barium niobate (CBN) [6], strontium tetra borate (SBO) [7], and strontium barium niobate (SBN) [8]. The random domain structure of unpoled SBN allows for broadband quasi-phase matching of wavelengths over the whole visible spectrum [9–11]. Due to the noncollinear phase-matching condition, the signal of the second harmonic wave is emitted either in a plane [8, 10], on a cone [10–13] or in form of a toroid [14]. It has also been demonstrated that noncollinear second-harmonic generation in SBN can be used to characterize femtosecond laser pulses [15–17]. As the angular spectrum of planar SHG is directly related to the domain distribution, this process can be used for so-called *k*-spectroscopy [18, 19] and to examine the switching behavior of ferroelectric domains [20–22].

SBN possess a needle-like domain structures along the crystal's polar axis [23] and shows a fractal-like pattern with a wide length scale at the polar-end faces [24,25]. These patterns exhibit an irregular spatial distribution because of the random domain size. Hence, a wide spectrum of χ^2 reciprocal *k* vectors is offered necessary to compensate for the phase mismatch of the phase velocities interacting inside the nonlinear volume. However, the reported domain widths in SBN crystals range in literature between a few nanometers and a few micrometers [11, 26, 27]. Due to this broad spectrum of domain widths, the SH emission patterns can look very different. Recently, the role of ferroelectric domain structure in SHG in random media like SBN has been discussed theoretically and numerically [28] but a systematic experimental investigation is still lacking.

In this paper, we study planar noncollinear SHG of ultrashort laser pulses in SBN with different degrees of domain disorder assuming a domain width which is normally distributed. The order of the domains is varied by electrical domain switching, leading to different short-range ordered nonlinear photonic crystals. This approach allows to control the degree of disorder, which can be analyzed using the SHG emission pattern. All results are compared with a model suggested by Le Grand et al. [29] for SHG in media with random domains, which allows us to determine the mean domain width and dispersion, and therefore the degree of disorder. We start with different unpoled crystals and measure the angular distribution of the SH emission. Then, the evolution of SHG distribution during domain reversal is examined and different degrees of domain disorder are achieved by further repoling steps. Finally, the wavelength sensitivity of SHG in a short-range ordered crystal is analyzed providing an unambiguous fingerprint of the domain distribution.

2. Model for SHG in disordered domain structures

SHG of light in a modulated χ^2 nonlinearity is a well-known quasi-phase matching (QPM) phenomenon. The SH intensity $I^{(2\omega)}$ can be calculated with the nonlinear wave equations in the undepleted pump approximation. It is worth to note, that this approximation is still valid for all experiments shown here, due to the smallness of the conversion efficiency which amounts to 0.2% at the best. The SH intensity is

$$I^{(2\omega)}(|\Delta\mathbf{k}|) \propto (I^{(\omega)})^2 d_{\text{eff}}^2 \left| \int_V g(\mathbf{r}) e^{-i\Delta\mathbf{k}\cdot\mathbf{r}} d^3\mathbf{r} \right|^2 , \tag{1}$$

with the fundamental intensity $I^{(\omega)}$, the phase mismatch $\Delta\mathbf{k} = \mathbf{k}^{(2\omega)} - 2\mathbf{k}^{(\omega)}$, and the effective nonlinear coefficient d_{eff}. The function $g(\mathbf{r})$ is a unitless function which describes the spatial modulation of the domains. Thus, a large SH intensity is produced for perfect phase matching

#143120 - $15.00 USD Received 24 Feb 2011; revised 29 Apr 2011; accepted 1 May 2011; published 26 May 2011

when $\Delta\mathbf{k} = 0$. This can be achieved for instance by birefringence phase matching. In a quasi-phase matching scheme the phase mismatch is compensated for by the corresponding Fourier components $\mathbf{G}$ of the modulation function $g(\mathbf{r})$ to achieve $\Delta\mathbf{k} = \mathbf{G}$. To fulfill the phase matching condition at a certain wavelength one can periodically pole the ferroelectric crystal in one dimension with the corresponding period. To enlarge the bandwidth quasi-periodic nonlinear photonic crystals can be designed [30]. However, even in periodically poled crystals due to a slightly disordered periodic structure, random quasi-phase matching becomes possible away from resonance [31].

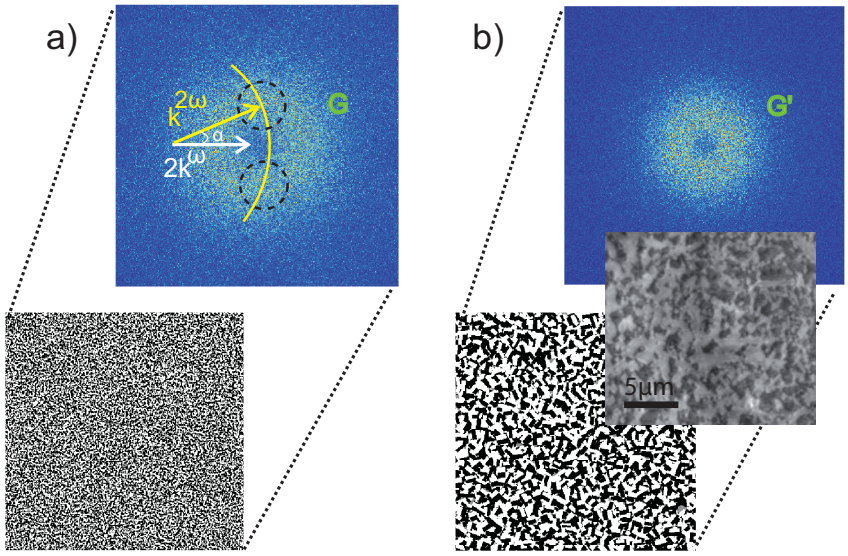

Fig. 1. Simulation of the spatial domain distribution and corresponding Fourier spectrum. The domains have a rectangular shape and are arbitrarily rotated around the c-axis that results in a fractal-like domain distribution. The widths of the domains are normally distributed with a mean width a and variance σ and half of the ferroelectric domains are inverted. In b) the domain width and dispersion are three times larger than the width and dispersion in a). Each Fourier spectrum consists of a broad ring. The dashed circles represent matching of the phase velocities of the fundamental and second harmonic beams. The inset in b) shows a phase contrast picture of a repoled crystal with an electrical field applied along the *c*-axis looking through the surface perpendicular to the *c*-axis.

Naturally, SBN crystals have a random or short-range ordered domain distribution depending on their poling state. The domain distribution of unpoled SBN is often described as fractal-like [25]. As the SH intensity is proportional to the square of the modulus of the Fourier transform of the domain modulation $g(\mathbf{r})$ (Eq. (1)), a real fractal distribution would result in a broad spectrum of reciprocal vectors $\mathbf{G}$. Figure 1 represents a modeling of such type of random fractal-like domains in two dimensions. The individual domains have form of rods with a quadratic shape with 4-fold symmetry [32]. The rod sizes are normal distributed as assumed in [29] with a certain mean width a and variance σ. These patterns are also randomly placed and oriented, and therefore resemble to form of fractals. Here, only the transverse plane of the structures is considered. The light propagates normally to this plane. Half of the domains are inverted represented by bright and dark colors, respectively. The 2D Fourier transformation of

#143120 - $15.00 USD Received 24 Feb 2011; revised 29 Apr 2011; accepted 1 May 2011; published 26 May 2011

this distribution (Eq. (1)) yields the χ^2 reciprocal vectors, used to match the phase velocities of the fundamental and the harmonic waves. The brightness represents the strength of the spectral components. The possible directions of the SH wave vector are presented by the yellow curve. The two intersections (marked with dashed circles) of the curve and the circle represent the region of quasi-phase matching. Hence, an inhomogeneous SH intensity distribution is expected even if the spatial domain distribution is fractal-like. On the contrary, unlike to the disordered structures, the lacking of *k* vectors needed for frequency doubling in single domain crystals at best leads to low conversion efficiencies. The inset in Fig. 1b) shows a phase contrast picture of a repoled crystal with an electrical field applied along the *c*-axis and looking through the surface perpendicular to the *c*-axis. The domains are randomly distributed and have fractal-like shape with typical dimensions on the order of μm.

To describe the SH intensity in a short-range ordered SBN crystal analytically we use a model described in [29] and theoretically analyzed in [28]. We assume that the domain width is Gaussian distributed with a mean value a and the variance (dispersion) σ. The Fourier spectrum of this spatial distribution remains a Gaussian distribution. Thus, for a small dispersion ($\sigma \ll a$) the SH intensity behind the crystal can be expressed as:

$$I^{(2\omega)}(|\Delta k|) \propto \frac{4N}{(|\Delta k|)^2} \frac{1-e^{-\sigma^2(|\Delta k|)^2}}{1+e^{-\sigma^2(|\Delta k|)^2}+2\cos(|\Delta k|a)e^{-\sigma^2(|\Delta k|)^2/2}}, \tag{2}$$

where N is the number of domains and $|\Delta k|$ is the phase mismatch, which can be calculated for every wavelength and emission angle α by the phase matching condition with the reciprocal grating vectors (Fig. 1):

$$|G| = (4|k^{\omega}|^2 + |k^{2\omega}|^2 - 4|k^{\omega}||k^{2\omega}|\cos\alpha)^{1/2}. \tag{3}$$

Equation (2) can be interpreted as the nonlinear diffraction at a strongly disturbed domain grating. For a small dispersion σ the SH intensity is mainly emitted into the first diffraction orders (nonlinear Bragg diffraction). With increasing domain dispersion these two Bragg peaks are becoming broader and move to smaller angles. Usually one will expect only a broadened zero order or in addition two broad SHG peaks around the zero order. To measure the degree of disorder we can determine the ratio of the dispersion and the mean width $R = \sigma/a$.

3. Experimental arrangement

For the investigation of the domain distribution, the second harmonic signal is directly scanned with a photodiode (Coherent OP-2 VIS) behind the crystal. For frequency conversion we use ultrashort laser pulses, generated by a laser system consisting of a mode-locked Ti:sapphire oscillator, a regenerative amplifier and an optical parametric amplifier. The repetition rate is 1 kHz, the pulse duration is about $\tau_p = 100$ fs, and the pulse energies are up to 150 μJ depending on the wavelength which is tuned in the experiments between 800 nm and 1500 nm. Nearly transform-limited Gaussian laser pulses ($M^2 \approx 1.2$) with a diameter of about 1.5 mm are propagating without focusing perpendicular to the *c*-axis of the SBN crystal. The light is always extraordinarily polarized addressing the largest electrooptic coefficient d_{33} of SBN. The SHG signal is emitted perpendicular to the *c*-axis in the plane of the fundamental beam as depicted in Fig. 2. Transmitted light of the fundamental beam is blocked by a combination of appropriate color and interference filters. To verify if the pulse duration has any influence on the spatial distribution of the SHG signal, a supplementary experiment has been carried out with ns-laser pulses at 1064 nm.

#143120 - $15.00 USD Received 24 Feb 2011; revised 29 Apr 2011; accepted 1 May 2011; published 26 May 2011

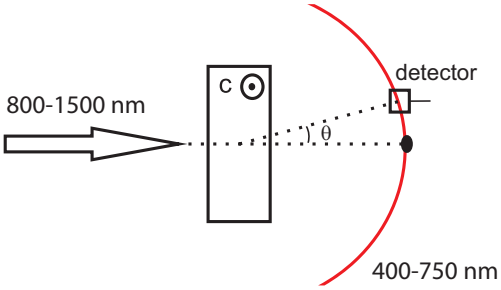

Fig. 2. Experimental setup for recording the SHG power behind the SBN crystal.

In order to avoid any differences between the domain distribution from one as-grown sample to another, and to present a consistent picture valid for all samples, the samples were initially heated above the Curie-Temperature $T_c \approx 70^\circ$ followed by cooling down without applying an electrical field. The domains are then strongly affected by poling the sample electrically at room temperature, providing the desired different degrees of domain disorder. In the experiments, we are using $Sr_xBa_{1-x}Nb_2O_6$ crystals grown by the Czochralski method with a congruently melting composition x = 0.61 [34] with different dimensions and dopants. Sample No. 1 ($3.5 \times 3.5 \times 1\ mm^3$) is doped with CeO_2 and the large surface parallel to the *c*-axis is polished to optical quality. Sample No. 2 is undoped ($5 \times 5 \times 5\ mm^3$) with all surfaces polished to optical quality. Sample No. 3 ($6.6 \times 6.6 \times 1.6\ mm^3$) is doped with Cr_2O_3.

Four types of experiments have been performed:

1. The second harmonic distribution was scanned up behind three unpoled samples with different sizes and doping. The samples were heated up above the Curie temperature to $\approx 200\ ^\circ C$ for 2 hours to avoid any spurious polarization and cooled down to room temperature.

2. To show the domain-distribution effect on the SH distribution, the spatial SH spectrum was scanned up during the poling process at room temperature.

3. Evolution of SH distribution was shown at different poling states, providing different degrees of domain disorder.

4. To check the wavelength sensitivity of the SH structure the SH distribution was measured over a wide range of fundamental wavelengths from $800 - 1500$ nm for two characteristic poling cases.

4. Experimental results and discussion

4.1. Overview of SHG for different poling states

We distinguish between four defined poling states, namely the *field cooled* state, where the crystal is heated up above the Curie temperature and cooled down to room temperature with an applied electrical field; the *unpoled* state, where the crystal is heated up above the Curie temperature and cooled down to room temperature without an applied electric field; the state, where the crystal is *poled* at room temperature by applying an electrical field above the coercive field, and the *repoled* state, where an unpoled crystal is first poled at room temperature and then repoled by applying an electrical field above the coercive field. Figure 3 shows experimental photographs of four characteristic frequency doubling processes of 1300 nm pulses, referring to different degrees of domain disorder in the SBN sample No. 1.

#143120 - $15.00 USD Received 24 Feb 2011; revised 29 Apr 2011; accepted 1 May 2011; published 26 May 2011

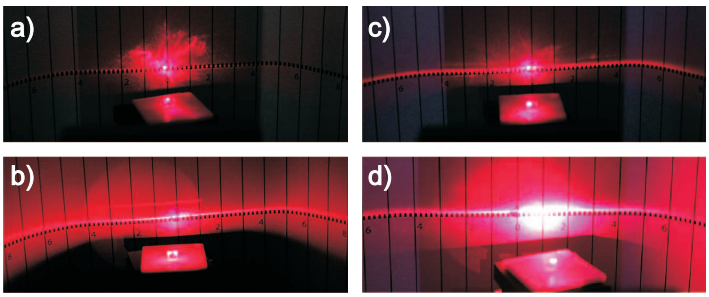

Fig. 3. Photographs of the SH emission on a screen behind the crystal for different poling states of the SBN crystal. The fundamental wavelength is 1300 nm and the pulse energy is about 135 μJ. a) field cooled, b) unpoled, c) poled at room temperature, and d) repoled at room temperature.

Figures 3a) and b) show the SHG intensity distributions and the corresponding reciprocal grating vectors variety after cooling down with an applied electrical field and without field, respectively. As clearly shown, in the field-cooling case the crystal is homogeneously poled, representing a single domain crystal. No wide intensity distribution behind the crystal can be observed due to the lack of small domains. On the other hand, after cooling down without an applied field, smaller domain sizes are available which cause a wide spatial SH distribution. The latter case will be studied in detail in the next section. Figure 3c) shows a different domain distribution induced by switching the crystal at room temperature. After cooling down, an electric field was applied and increased stepwise until finally 4.7 kV/cm was reached. The step size was increased by 10 V/cm per second in all experiments. In contrast to the field cooling switching, the poling at room temperature does not induce a single-domain crystal because pinning charges destabilize the domains, i.e. some domains flip back. Thus, a wide SH distribution is still emitted but weaker than in the unpoled case. As a quantity defining the distribution of the domain orientation, the spontaneous polarization P_s can give a global estimation. As well known, in case of an unpoled crystal, the spontaneous polarization amounts to zero, indicating the domains are statistically distributed, and the number of the inverted domains in the two possible orientations is approximately the same. The importance of the role of the spontaneous polarization comes from the fact, that the second harmonic distribution depends on the domain distribution. This connection becomes clear when measuring the polarization after poling the crystal in different ways. For the field cooling case, P_s amounts to 30 $\mu C/cm^2$, leading to a single domain crystal. On the other hand, P_s calculated from the repoling displacement current is ≈ 27 $\mu C/cm^2$ for the case of poling at room temperature. A smaller P_s implies that the crystal was partially poled. This effect results in the SH spatial spectrum. It is worth to note that in case of periodically-poled samples with a duty cycle of one, the polarization is equal to zero, too. Repoling the crystal further increases the SHG efficiency from 0.06% for the unpoled case to 0.2% for the repoled case and the SHG distribution becomes narrower (Fig. 3d)).

#143120 - $15.00 USD Received 24 Feb 2011; revised 29 Apr 2011; accepted 1 May 2011; published 26 May 2011

4.2. *SHG in three different unpoled samples*

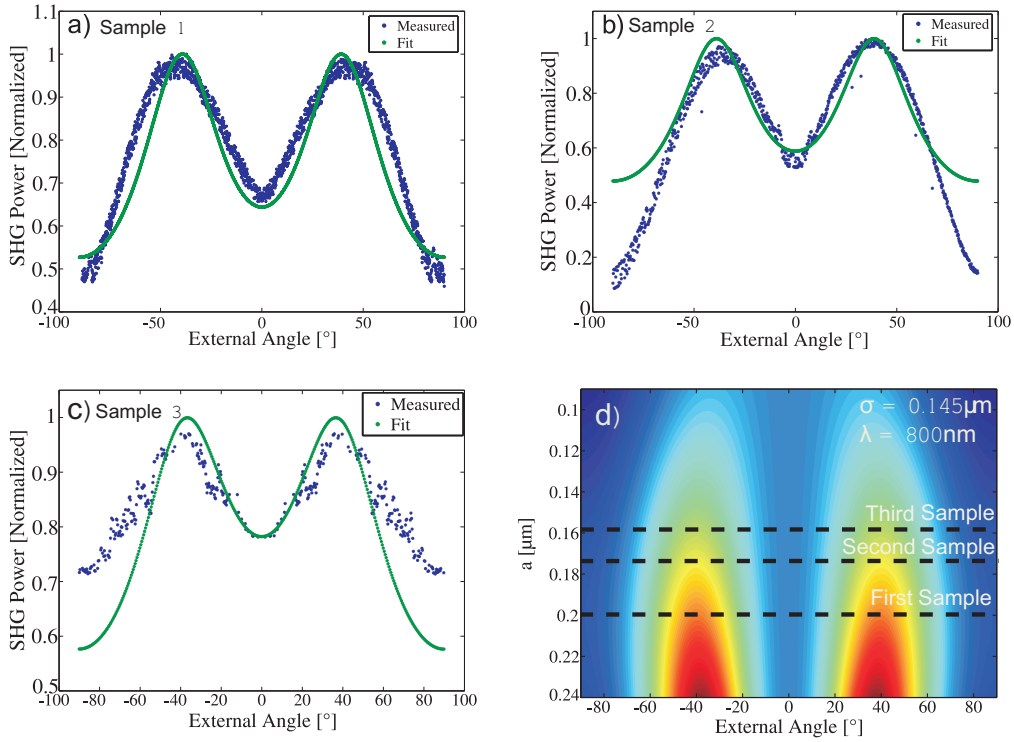

Fig. 4. a)-c) Normalized SH intensity distribution for a fundamental wavelength of 800 nm and an average power of 150 mW for three different unpoled SBN samples, indicating similar domain distributions. The lines are fits of Eq. (2) to the experimental data. d) Calculated mean domain width a in dependence of SH scattering angle according to Eq. (2) for a fixed wavelength and domain dispersion. The dashed lines represent the fit parameters of the three samples.

As the domain distribution of SBN typically strongly depends on the history of poling and heating procedures, we want to induce an almost random domain distribution in three different samples to prevent this situation, and look for the SHG distribution. Therefore, the three samples No. 1, No. 2, and No. 3 were heated up above the Curie temperature to 200 °C for about two hours and cooled down to room temperature. The measured SH intensity distributions for 800 nm pulses are depicted in Figs. 4a) to c). It can be seen that the SH intensity distribution in all samples nearly look the same with two distinct wide peaks around $\approx 45°$. If we heat the crystals up to higher temperatures at about 650 °C, the SH intensity distribution at room temperature still looks the same. Therefore, at 200 °C, all memories in form of pinning charges are erased. The SH intensity distribution also does not change if we are using ns-laser pulses instead of fs-laser pulses. Hence, we can neglect any influence of ultrashort laser pulses like the group velocity dispersion on the SH intensity distribution. All following experiments are carried out with fs-laser pulses. The two broad SHG peaks clearly indicate a comparable domain distribution in all three unpoled samples. Its remarkable that the domain distribution in unpoled SBN crystals is independent of the crystal size and dopants.

The typical mean domain widths a and variances σ can be determined for the three unpoled samples using Eq. (2). The lines in Figs. 4a) to c) are fits of Eq. (2) to the experimental values.

#143120 - $15.00 USD Received 24 Feb 2011; revised 29 Apr 2011; accepted 1 May 2011; published 26 May 2011

The mean domain widths a and variances σ are $a = 0.2$ μm and $\sigma = 0.145$ μm for sample No. 1, $a = 0.175$ μm and $\sigma = 0.145$ μm for sample No. 2, and $a = 0.158$ μm and $\sigma = 0.145$ μm for sample No. 3. In Fig. 3d) the predicted angular distribution in dependence of the domain width a for a fixed dispersion of $\sigma = 0.145$ μm is plotted. The dashed lines represent the phase matching conditions for the three samples. However, the evaluated sizes also match the sizes measured in [25–27].

The dependence of the SHG intensity distribution on the input power is presented in Fig. 5a). The SHG intensity is symmetrically distributed and increases continuously with increasing input power. This increase follows a quadratic behavior as can be seen in Fig. 5b), where the SHG power at five different angles, representing the five characteristic turning points, is plotted versus the input power. The lines are quadratic fits according to Eq. (1). Figure 5 clearly shows that the angular distribution of the SH signal is independent of the input power.

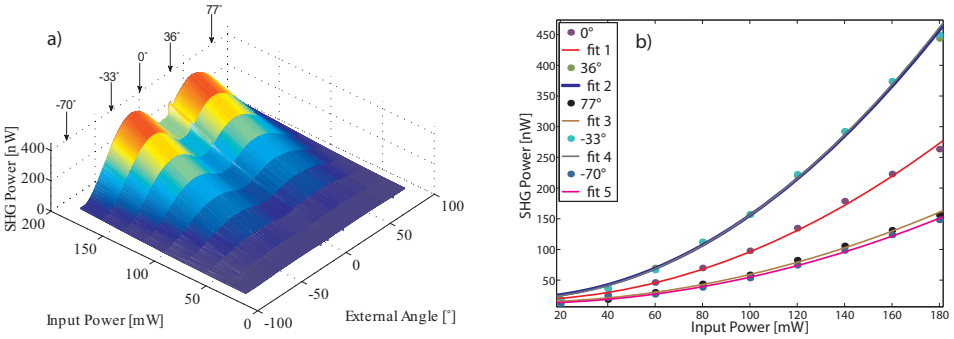

Fig. 5. a) SH intensity distribution in dependence of input power at 800 nm; b) SHG power at five different angles in dependence of input power. The lines are quadratic fits.

4.3. Evolution of the SHG distribution during domain reversal

Now, a closer analysis of the domain role is directly performed through scanning the SH angular intensity while poling crystal No. 1 at room temperature. Figure 6 shows that increasing the applied electrical field above the coercive field leads to a shift of the peaks to smaller angles until they disappear at 2400 V/cm and one peak arises in the middle, indicating that the crystal is poled even though not completely, as already seen in the previous section. In [19] it was pointed out, that the electrically switching leads to an increase of the domain structures at the expense of the density of smaller domains. Thus, domain sizes shift from small to large scale. In order to show the intensity distribution only, the results are normalized, taking into account, that the SH intensity also shows a peak around the field $E \approx 1300$ V/cm for this unpoled SBN [19].

At the end of the poling process the SH pattern has a characteristic shape as can be seen in Fig. 7, meaning that a dramatic change happened during the poling process. To evaluate the domain size Eq. (2) is fitted to the experimental data. The domain sizes experience uniform growth from $a = 0.2$ μm to $a = 3.1$ μm, accompanied with a slightly growth of dispersion $\sigma = 0.58$ μm.

#143120 - $15.00 USD Received 24 Feb 2011; revised 29 Apr 2011; accepted 1 May 2011; published 26 May 2011

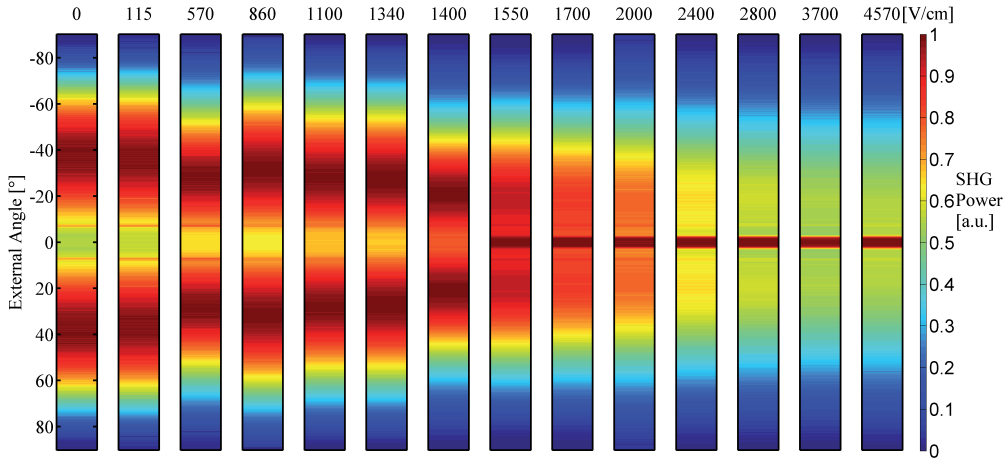

Fig. 6. Measurements of SH pattern during the poling process at 800 nm and input power of P = 150 mW by applying an electrical field at room temperature. The distinct peaks, which appear when no field is applied disappear at 2400 V/cm, producing one peak in the middle.

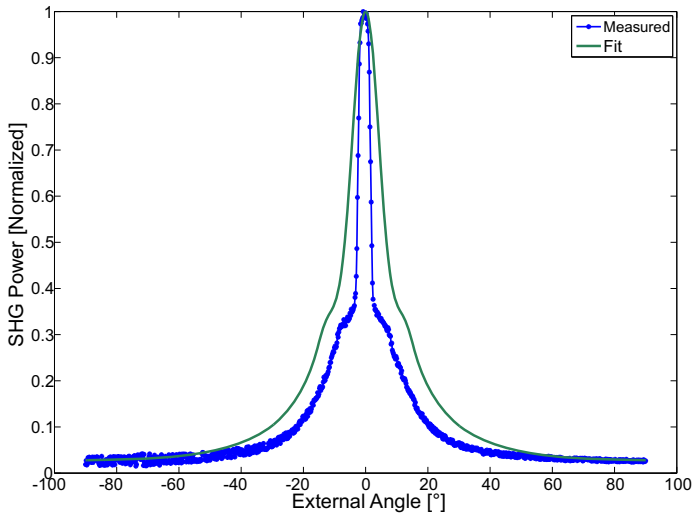

Fig. 7. Scan of the SH pattern at the end of the poling process at 800 nm (see also SH intensity distribution in Fig. 6 at $E = 4570\,\mathrm{V/cm}$). Domain sizes are greatly affected and become larger. The fitted width and dispersion are $a = 3.1$ μm and $\sigma = 0.58$ μm, respectively.

#143120 - $15.00 USD Received 24 Feb 2011; revised 29 Apr 2011; accepted 1 May 2011; published 26 May 2011

4.4. *SHG for different degrees of disorder*

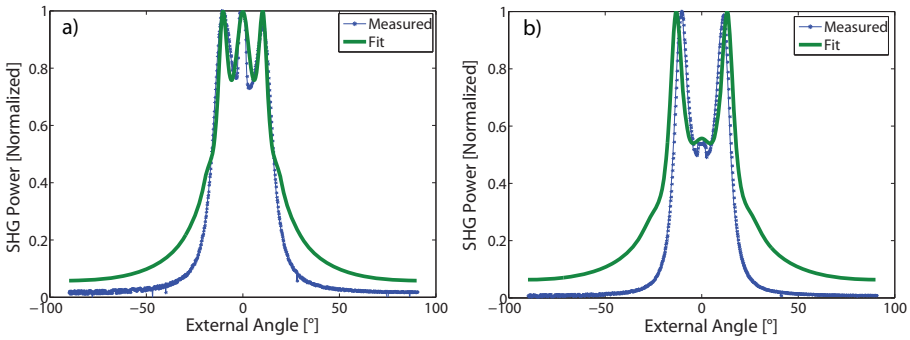

Fig. 8. a) Scan of the SH distribution of 800 nm for 150 mW input power after the first repoling (blue curve) and the corresponding fit (green curve) with $a = 3.64$ μm and $\sigma = 0.5$ μm; b) scan after the second repoling (blue curve) and the corresponding fit (green curve) with $a = 3.8$ μm and $\sigma = 0.5$ μm.

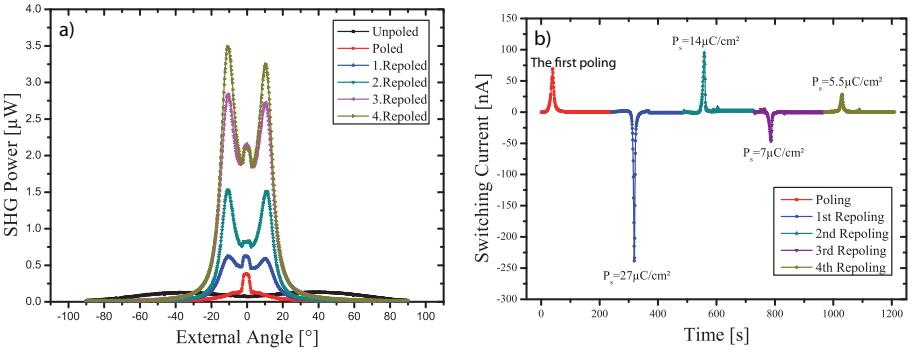

Fig. 9. a) Scans of SH distribution when further repoling the crystal. Both peaks experience no significant change more, but become sharper; b) The corresponding displacement current of the repoling processes. The measured spontaneous polarization is shown.

Different degrees of domain disorder are achieved by further repoling the crystal. The growing of the domains is observed and scanned as shown in Fig. 8. The corresponding fit parameters are: for the first repoling (Fig. 8a): $a = 3.64$ μm and $\sigma = 0.5$ μm and for the second repoling: $a = 3.8$ μm and $\sigma = 0.5$ μm. It is worth noting, that no further significant changes are observed in the SH distribution when the crystal is further repoled, except that the two peaks become sharper and the transmitted peak disappears as can bee seen in Fig. 9a. The ratio $R = \sigma/a$, which defines the disorder degree here, decreases from $R = \sigma/a = 0.83$ for the unpoled sample to $R = \sigma/a = 0.13$ for the repoled sample. The small value of R clearly points to some kind of domain order in the sample. Thus, in the unpoled sample as well as in the repoled sample the ferroelectric domains are distributed in a short-range order and not in a completely random order. However, the repoled sample has a higher degree of order compared with the unpoled one and such a 2-dimensional nonlinear photonic crystal with a short-range order can be used for broadband SHG which will be shown in the next section. Regarding the SH distribution similar SH structures can be found in domain inverted $LiNbO_3$ crystals with a short-range order [33].

#143120 - $15.00 USD Received 24 Feb 2011; revised 29 Apr 2011; accepted 1 May 2011; published 26 May 2011

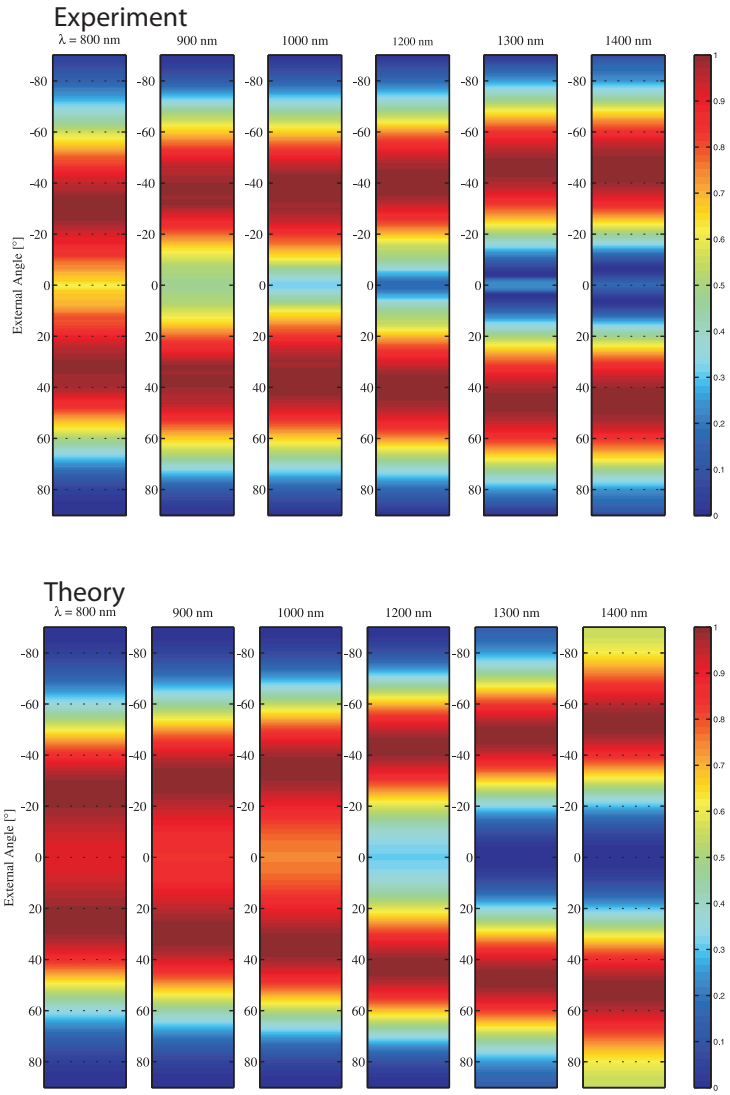

Fig. 10. Scans of SH distribution of a wide range of input wavelengths from 800 – 1400 nm for an unpoled SBN (top). At larger wavelengths the peaks move out. This is confirmed theoretically (bottom).

While the degree of domain disorder stays the same after the second repoling the total SH intensity increases with every repoling cycle (see Fig. 8). This is accompanied with a decreasing spontaneous polarization P_S. The measurements of the poling current, shown in Fig. 9b), denote a dramatically decay of the spontaneous polarization after each domain switching. This aging effect leads to a state where the domains cannot be further switched. In general the SH intensity is maximal when the polarization is zero, i.e. at the maximum of the poling current. Then, the number of domains pointing in the minus and plus *c* direction are the same. During a poling process this duty cycle changes and therefore the total SH intensity changes, too.

#143120 - $15.00 USD Received 24 Feb 2011; revised 29 Apr 2011; accepted 1 May 2011; published 26 May 2011

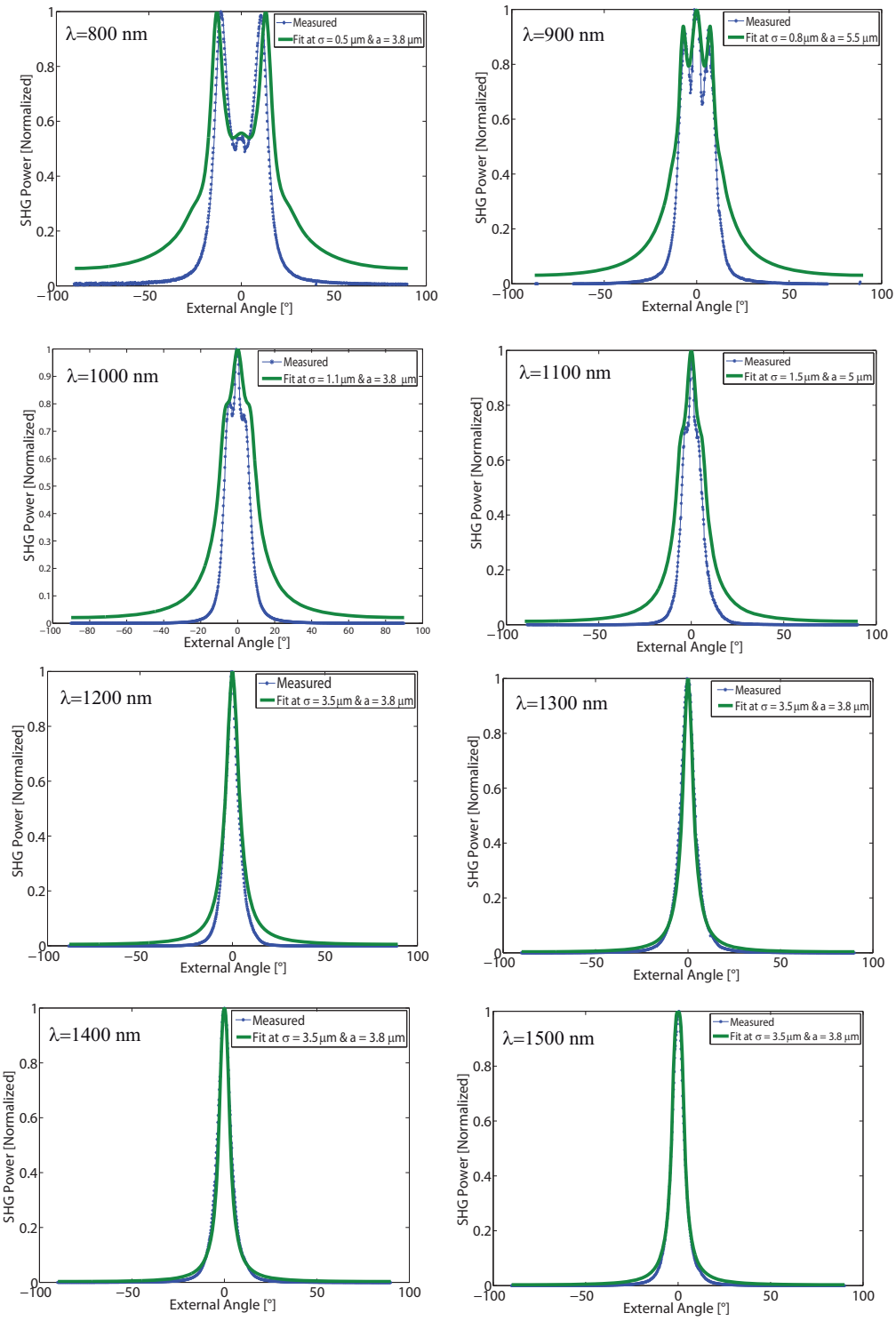

Fig. 11. Scans of SH distribution of a wide range of input wavelengths from 800 – 1500 nm for a two-times repoled SBN. This complex behavior is also confirmed theoretically.

#143120 - $15.00 USD Received 24 Feb 2011; revised 29 Apr 2011; accepted 1 May 2011; published 26 May 2011

4.5. *Wavelength sensitivity of the SH patterns*

In the present experiment the wavelength dependence for two characteristic domain distributions is analyzed. First, the SH intensity distribution is scanned behind an unpoled SBN crystal for fundamental waves from 800 to 1400 nm. The normalized intensity scan is shown in Fig. 10. The intensity maxima move out from $\approx 30^\circ$ to 50° with increasing wavelength. The domain distribution has a mean width of $a = 0.2$ μm and dispersion of $\sigma = 0.145$ μm. In good agreement this behavior is clearly introduced theoretically and the angular shift is estimated to be about $\approx 20^\circ$ for the intensity maxima as shown in Fig. 10 (bottom).

Second, the measurements show a more remarkable wavelength dependence in the case of a two-times repoled SBN crystal. The SH peaks, lying at $\approx 20^\circ$ at 800 nm (Fig. 11), experience a deformation, combined not only with a growing of the central peak, starting from 900 nm, but also localizing the entire SH spectrum. The two peaks then start to vanish until they completely disappear at 1200 nm, producing a localized SH angular intensity from 1200 to 1500nm. In order to mimic this structures the model is used in the same manner. But in this case, to get the best fit for each wavelength we had to modify the distribution parameters a and σ slightly. However, for all wavelengths the determined domain diameters are in the range of 3.8 μm $\pm$ 3.6 μm.

As can be seen in Figs. 7, 8 and 11 there are always some deviations between the fits and the experimental values. We attribute these deviations to the limitations of the used model. The model assumes a one-dimensional domain distribution whereas the domains in SBN are distributed in two dimensions. Nevertheless, we take this into consideration by implementing a two-dimensional phase matching condition (Eq. (3)). Furthermore, it is assumed that the domain width is normally distributed. For as grown SBN crystals such a Gaussian domain distribution has been verified [11], but the statistics of domain distribution might be different for SBN crystals which have been treated with an external electrical field. Finally, the model is valid for a small variance ($\sigma \ll a$) only and in our SBN crystals the variance is still large. However, in spite of these limitations the model yields reasonable domain diameters and variances for a large range of wavelengths and for different poling states of the crystals.

5. Conclusions

We have studied noncollinear planar SHG in strontium barium niobate with different degrees of domain disorder. Analyzing the angular distribution and wavelength dependence of the second harmonic emission pattern, the mean width and dispersion of domains can be determined taking into account a normal distribution of domains. SBN crystals which have been heated up above the Curie temperature and cooled down to room temperature exhibit the strongest degree of disorder with mean domain widths on the order of 160 nm. The corresponding SHG distribution is spatially broadened with two distinct broad peaks at around 45° depending on the wavelength. During the first poling the domain width increases and the two broad peaks move to smaller angles merging finally into one central weak SHG peak. Now, almost all domains are orientated in the same direction and the polarization has its maximum value. Further repoling of the crystal leads to a smaller polarization due to the aging effect. As the modulation of the orientation of the domains increases the SHG efficiency also increases with every further repoling step. Hereby we have produced a two-dimensional nonlinear photonic crystal where the domains are distributed in a short-range order. Such a crystal has a broad SHG bandwidth and we expect an efficient generation of the third and fourth harmonic via a cascading effect. The degree of domain disorder of the nonlinear photonic structure can be determined from the ratio of the dispersion and mean domain width and the measurement of the wavelength sensitivity of the SHG distribution unambiguously reveals the degree of domain disorder. This nonlinear spectroscopy can be used in any kind of nonlinear photonic structure like periodically poled

#143120 - $15.00 USD Received 24 Feb 2011; revised 29 Apr 2011; accepted 1 May 2011; published 26 May 2011

crystals to map the disorder in nonlinearity.

Acknowledgment

We thank Prof. Dr. K. Betzler and Dr. U. Heine from the University of Osnabrück for experimental support and fruitful discussions. Financial support of Deutsche Forschungsgemeinschaft and Open Access Publication Fund of University of Münster is gratefully acknowledged. M. A. acknowledges financial support of the University of Damascus.

#143120 - $15.00 USD Received 24 Feb 2011; revised 29 Apr 2011; accepted 1 May 2011; published 26 May 2011